A&A 376, 484–488 (2001)
DOI: 10.1051/0004-6361:20010922


Astronomy & Astrophysics

# A disrupted molecular ring in planetary nebula G119.3+00.3 (BV 5-1)⋆

E. Josselin[1] and R. Bachiller[2]

[1] GRAAL–CC72, UMR 5024–ISTEEM, CNRS/Univ. Montpellier II, 34095 Montpellier Cedex 05, France
[2] Observatorio Astronómico Nacional (OAN), IGN, Apartado 1143, 28800 Alcalá de Henares, Spain

Received 27 April 2001 / Accepted 26 June 2001

**Abstract.** New, high-sensitivity interferometric CO observations of BV 5-1 show that the molecular gas in this bipolar planetary nebula is distributed along a very inhomogeneous ring made of clumps. The individual masses of such molecular clumps are $\sim 10^{-4}$ $M_{\odot}$. The BV 5-1 molecular ring is seen edge-on, it is nearly perpendicular to the axis of bipolarity of the nebula, and it is expanding with an expansion velocity of $\sim 9$ km s$^{-1}$. BV 5-1 is confirmed to be a relatively evolved nebula, as indicated by both its kinematic age ($\sim 2.4 \times 10^4$ yrs) and its molecular to ionized mass ratio ($\sim 0.3$). The structure of the BV 5-1 molecular ring, as well as that of other rings previously observed in a few additional nebulae, underscore the importance of strongly asymmetrical mass loss processes starting early at the asymptotic giant branch phase.

**Key words.** planetary nebulae: general – planetary nebulae: individual: BV 5-1 – radio lines: ISM – stars: mass loss

## 1. Introduction

Since the discovery of CO emission in a planetary nebula (PN; Mufson et al. 1975), molecular gas has been widely detected in PNe (e.g. Huggins et al. 1996) and especially in bipolar PNe (Kastner et al. 1996). The study of this molecular gas component through the emission of CO rotational lines has provided key informations for the understanding of these evolved objects. Indeed, the nebular molecular gas must originate in the mass loss during the precursor phase, the asymptotic giant branch (AGB). It is then gradually dissociated and ionized as the central star warms up, so that the ratio between molecular mass and ionized mass ($M_{\rm m}/M_{\rm i}$) provides an (almost) distance-independent evolutionary stage indicator (Huggins et al. 1996; Josselin et al. 2000a). Furthermore, the very high spectral resolution provided by millimeter wave spectroscopy brings strong constraints on the dynamics and shaping of PNe.

Until recently, the shaping of PNe was believed to proceed through the interaction of two winds, the slow ($\sim 10$ km s$^{-1}$) dense wind ejected on the AGB and a faster tenuous and isotropic wind flowing during the proto-PN phase. Yet, recent observations put in evidence high velocity collimated outflows in an increasing number of PNe (Sahai & Trauger 1998; Forveille et al. 1998). The generation of this kind of outflows requires ingredients such as rotation of the central star, accretion disks around binary systems, or significant magnetic fields (see Różyczka & Franco 1996 and the recent review by Frank 2000). The formation of a gaseous ring around rotating AGB stars, and the subsequent evolution of the nebula to a bipolar PN has been described by García-Segura et al. (1999).

Because of its faintness, the fine bipolar structure of BV 5-1[1] has been only recently discovered (Manchado et al. 1996; see also Fig. 1a in Guerrero et al. 2000). BV 5-1 is a highly enriched type I PN. Its optical images are dominated by a bright equatorial lane perpendicular to the nebular symmetry axis. CO $J = 1$–0 and 2–1 emission was recently detected in BV 5-1 by Josselin et al. (2000a), but the CO emission was hardly resolved in the 2–1 line with the $10''$ beam of the IRAM 30-m telescope. The CO emission seemed to approximately extend along the E-W direction, thus in agreement with the bright part

*Send offprint requests to*: E. Josselin,
e-mail: josselin@graal.univ-montp2.fr

⋆ Based on observations carried out with the IRAM Plateau de Bure Interferometer. IRAM is supported by INSU/CNRS (France), MPG (Germany) and IGN (Spain).

[1] "BV 5-1" refers to the first entry of Table 5 ("New planetary nebulae") in Böhm-Vitense (1956). This nebula is also often designed as BV-1 or BV 1. Its name according to the standardized designation for PNe is PN G119.3+00.3.

of optical images, but the structure of the molecular envelope was not studied in detail due to the relatively poor resolution of such observations. We report here new interferometric images of BV 5-1 in the 1–0 and 2–1 lines of CO providing a resolution of $\sim 2''$. The new images reveal that the molecular envelope consists of an expanding ring which is being disrupted by the radiation and winds from the central star.

## 2. Observations

Interferometric observations, centered on BV 5-1 ($\alpha_{J2000} = 00^h19^m59.3^s$, $\delta_{J2000} = +62°59'00''$) were made with the IRAM interferometer (Plateau de Bure, near Grenoble, France; Guilloteau et al. 1992) on 1995 August 15th and 24th. We observed simultaneously the two CO $J = 1$–0 and 2–1 lines (115.271 and 230.538 GHz, respectively) with two compact configurations of the array, which consisted of four 15-m antennas. Observing conditions were good, with a seeing varying from 0.4 to $1.5''$. The RF passband and amplitude were calibrated using MWC349 (flux = 1.70 Jy at 230 GHz) and the phase calibration was performed using 1928+738 (0.57 Jy).

No single-dish observations as zero-spacing data were added to these observations. First, this should not be necessary for such a compact source (size $\lesssim 18''$) and this was confirmed by the measured total flux, compared to the one we measured at the IRAM 30 m telescope (see Sect. 3.1 and Josselin et al. 2000a). Second, some points of our single-dish observations probably suffered from slight pointing problems, so the spatial resolution would have probably been degraded with such an operation.

Data reduction was performed with the GILDAS software, developed at IRAM and Grenoble Observatory. It included calibration of passband, phase and amplitude, map restoring and CLEANing with the CLARK method. The restored gaussian clean beams for the CO 1–0 and 2–1 observations are $4.76'' \times 4.46''$ at a position angle of 36° and $2.7'' \times 2.13''$ at a position angle of –30°, respectively.

As a by-product of these observations, an upper limit of 1 mJy was derived for the continuum emission of the nebula, which was not detected in any band. When compared to the upper limit measured at 5 GHz from VLA observations (<0.5 mJy; Aaquist & Kwok 1990), we conclude that the radio continuum spectrum from BV 5-1 is consistent with free-free Bremsstrahlung emission ($S_\nu \propto \nu^{-0.1}$).

The CO 1–0 emission is potentially contaminated by the recombination line H38$\alpha$, as both frequencies are separated by only 3 MHz (Bachiller et al. 1992). However, the H38$\alpha$ line seems to be quite weak in BV 5-1, since the CO 2–1 profile agrees well with that of the CO 1–0 + H38$\alpha$ blend (Josselin et al. 2000a). Anyhow, since the newly obtained CO 2–1 map has much better spatial resolution than the 1–0 map, the following discussion is mainly based on the 2–1 line, which moreover does not suffer from any potential contamination.

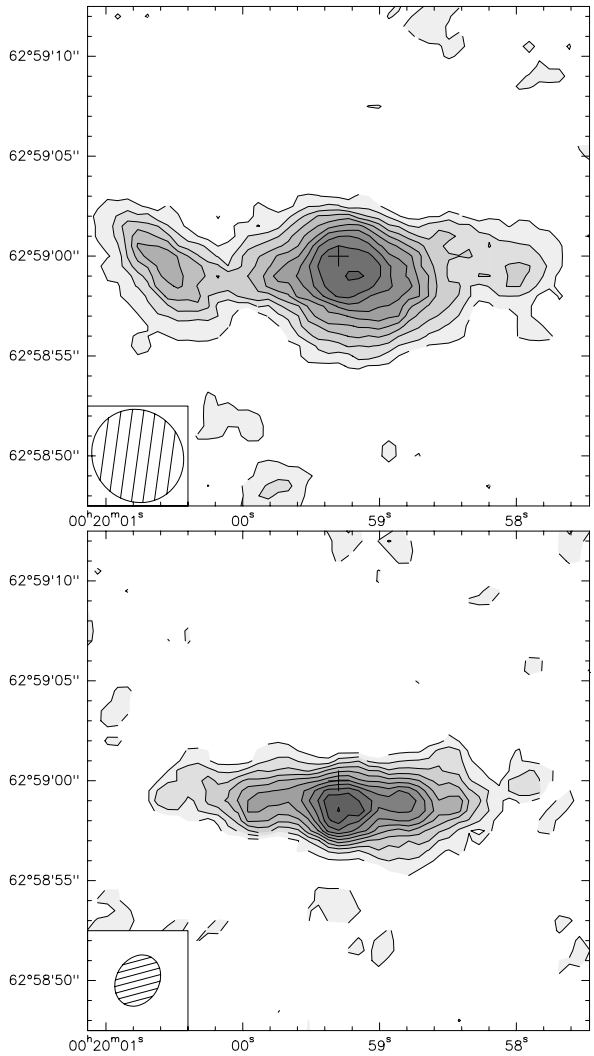


**Fig. 1.** Top panel: contour map of the integrated $^{12}$CO(1–0) emission from BV 5-1 over the whole velocity range of emission. The lower level contour and the contour spacing are 0.15 Jy beam$^{-1}$ km s$^{-1}$. Bottom panel: contour map of the integrated $^{12}$CO(2–1) emission from BV 5-1 over the whole velocity range of emission. The lower level contour and the contour spacing are 0.4 Jy beam$^{-1}$ km s$^{-1}$. In both panels, the beam after cleaning is shown in the box in the lower left corner. The cross indicates the central position adopted for the observations.

## 3. Properties of the envelope

### 3.1. Overall structure

The overall distribution of the molecular gas as observed in the CO 1–0 and 2–1 lines are shown in the velocity-integrated maps in Fig. 1. From the map in the 2–1 line, we measure that the molecular emission extends over a bar of angular diameter $\sim 20''$ and total area $70''^2$. Assuming a distance of 5.5 kpc and an expansion velocity of 10 km s$^{-1}$ (Josselin et al. 2000a), this corresponds to a linear size of $\sim$0.5 pc and a kinematic age of $\sim 2.4 \times 10^4$ yr. This latter estimation must be considered as a lower limit to the actual age of the nebula, since CO is very

probably highly photodissociated, so that the nebular size is underestimated.

As we will show in the next section, this bar is in fact the projection of a ring seen almost perfectly edge-on. It coincides quite well with the lane observed in optical images (Guerrero et al. 2000), and in particular with the brightest part of the $H_2$ image at 2.12 $\mu$m, the location of local maxima being in good agreement. The most noticeable difference is the warped extension of this lane which does not appear on our CO maps. We stress that the near infrared $H_2$ emission arises from material which is hotter (a few $10^3$ K) than that emitting the low-$J$ CO lines (which probably is below $10^2$ K). Thus the $H_2$ emission very likely delineates the thin external skin of the dense clumps which is heated by the central star, whereas the CO lines trace the bulk of the cold molecular material inside the clumps. In summary, although the $H_2$ and CO lines are formed in regions which are closely related, it is not surprising to see that the corresponding maps are not perfectly coincident.

The morphology observed in the new interferometric map is slightly different from that observed by Josselin et al. (2000a). In particular there was a weak extension towards the northern direction in the single-dish data which is lacking in the new image. Such small differences can be attributed to slight pointing errors in the previous single-dish observations, since the mapping procedure of a so small source with a relatively large beam is very sensitive even to very minor pointing unaccuracies. The total CO flux and derived parameters were thus probably slightly overestimated in Josselin et al. (2000a), so we provide here more precise estimates of these parameters.

We have measured a total CO 2–1 flux of 21 Jy km s$^{-1}$, corresponding to a column density of $4.3 \times 10^{15}$ cm$^{-2}$. This estimate was done by assuming that the emission is optically thin, which is a plausible assumption as indicated by the high CO 2–1/1–0 intensity ratio (note that this ratio should be close to 1 in the optically thick limit). We also assumed an excitation temperature of 70 K, but the result depends only slightly on this value (Huggins et al. 1996).

In order to estimate the total mass of the molecular gas we need to assume a value for the CO abundance. Unfortunately, no meaningful upper limit for carbon abundance could be derived by Kaler et al. (1988) from their detailed composition study. However, it is worth noting that no strong $^{12}$C enrichment is expected in BV 5-1, since the high nitrogen abundance should reflect conversion of $^{12}$C into $^{13}$C and $^{14}$N during the hot-bottom burning phase. It seems hence reasonable to adopt a solar abundance for C. In addition, we have assumed that all C is in the form of CO within the dense clumps, so that the CO abundance with respect to $H_2$ is $[CO]/[H_2] = 3 \times 10^{-4}$. In fact this value is an upper limit to the actual average value, since CO could be partially photodissociated at least in the more external layers of the clumps. Nevertheless, under these assumptions, we derive a mass for the molecular gas component $M_m \simeq 2.8 \times 10^{-2}\ M_\odot$. Combined with

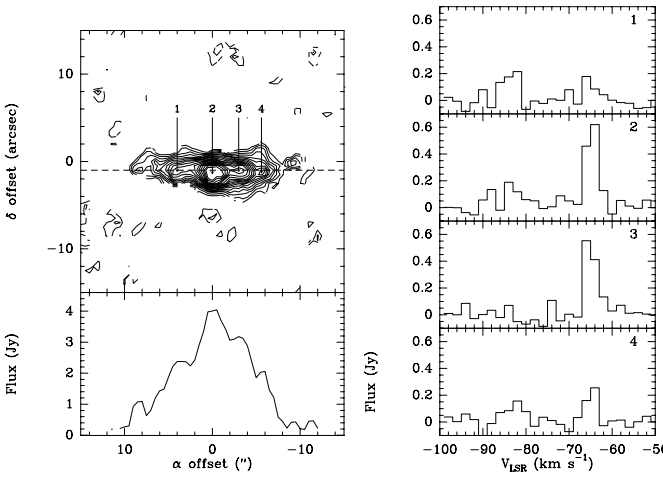


**Fig. 2.** Left panel: contour map of the integrated $^{12}$CO(2–1) as shown in Fig. 1; the horizontal dashed line indicates the cut from which the flux profile given below and the velocity-position diagram were obtained. Right panel: spectra extracted from the four positions labeled on the left panel and corresponding to the local maxima along the ring.

a mass of the ionized component $M_i \lesssim 0.1\ M_\odot$ (Gathier 1987; Josselin et al. 2000a), this gives a $M_m/M_i$ ratio $\gtrsim 0.3$. Note that if the actual CO abundance were lower that this assumed value, the molecular mass would be correspondingly higher, which would make the $M_m/M_i$ ratio somewhat higher than the estimate provided here. In any case, and in agreement with its kinematic age (see below), the value of the $M_m/M_i$ ratio indicates that BV 5-1 is a rather evolved object.

We display in Fig. 2 the flux profile obtained from a cut along the major axis of the "bar". It clearly appears very irregular, with some local maxima. The spectra observed towards each of the maxima show that the emission arises from a few discrete well-defined condensations or clumps, each one with relatively low internal velocity dispersion ($\sim$6 km s$^{-1}$). We next analyze in more detail this complex kinematic structure.

### 3.2. Kinematic structure

Figure 3 displays a velocity-position diagram built from the cut indicated by a dashed line in Fig. 2. The overall structure is well explained if the emission arises from a very inhomogenous expanding ring. This is indeed compatible with the previous observations by Josselin et al. (2000a), with apparently a slightly lower expansion velocity, $\sim$9 km s$^{-1}$. But, as the velocity resolution has been degraded to 2 km s$^{-1}$ (see also Fig. 4) because of the relative faintness of the nebular emission, this value remains fully compatible with that found from millimeter single-dish observations (10 km s$^{-1}$) and from the optical 658.3 nm NII line (11 km s$^{-1}$; Kaler et al. 1988). This coincidence between expansion velocities of the ionized and molecular gas indicates that the central part of the ionized nebula results from the photoionization of the molecular

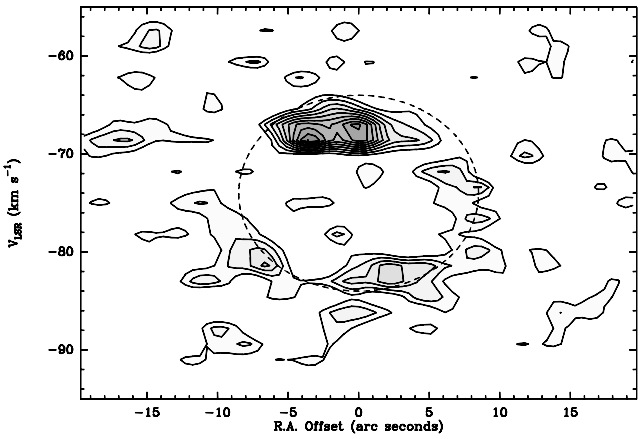


**Fig. 3.** Velocity-position diagram in the $^{12}$CO(2–1) obtained from the cut indicated in Fig. 2. The lower level contour and the contour spacing are 0.57 Jy beam$^{-1}$. The dashed ellipse recalls the overall structure found by Josselin et al. (2000a).

ring, as expected for this evolved PN. This ring is apparently seen edge-on and relatively thin, so that one cannot get direct informations on the ring size along the direction perpendicular to the plane of the sky. No hints of rotation are observed in the velocity field. So we conclude that a circular, non-rotating, clumpy ring is the best interpretation of the present observations.

The strong inhomogeneities found in Fig. 2 are better distinguished in the velocity-position diagram of Fig. 3. Two red-shifted clumps largely dominate the emission in this diagram and correspond to positions 2 and 3 in Fig. 2. Weaker clumps are distributed along the blue-shifted part of the ring. No obvious symmetries between clumps with respect to the center of the ring are perceived.

Each of these clumps can be individually identified in the channel maps of Fig. 4. Most of the emission is concentrated in a few velocity channels, around −83 km s$^{-1}$ and −64 km s$^{-1}$, and correspond to four unresolved clumps. The mass of each of these clumps is $\sim 10^{-4}$ $M_{\odot}$.

## 4. Discussion and conclusions

Rings of molecular gas, as this observed in BV 5-1, could be relatively common in bipolar PNe. In fact, similar geometries have been previously observed towards the young PNe M 2-9 (Zweigle et al. 1997), KjPn 8 (Forveille et al. 1998) and M 1-16 (Huggins et al. 2000). In all these cases, the orientation of the bipolarity orthogonal to the plane of the ring indicates interactions between an accelerated outflow and a slowly expanding envelope. Furthermore the ring systematically appears clumpy, and in some cases (e.g. M1-16) the clumps are placed in a clear symmetrical manner with respect to the central star, indicating the presence of strong interactions with jets close to the equatorial plane. As noted in the previous section, no obvious symmetry between clumps is observed in BV 5-1, but this could be due to the more advanced degree of evolution of this nebula with respect to the particularly young nebula M 1-16.

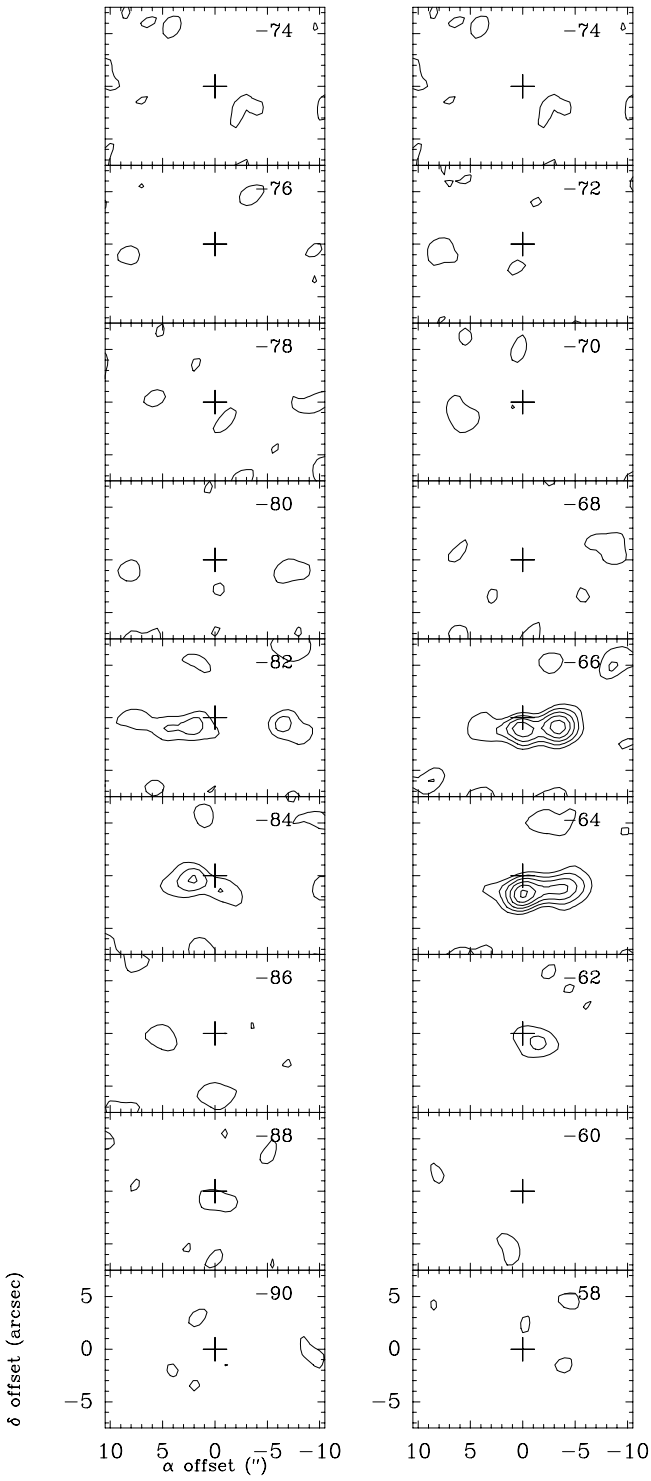


**Fig. 4.** Contour map of the $^{12}$CO(2–1) emission integrated over equally spaced velocity channels with width of 2 km s$^{-1}$. The left column corresponds to the blue-shifted emission and the right column to the red-shifted emission. In each column the top panel displays the emission at the central velocity (−74 km s$^{-1}$). The lower level contour and the contour spacing are 0.1 Jy beam$^{-1}$ km s$^{-1}$. The central LSR velocity for each panel is indicated in the top right corner.

The expansion velocities of such rings are always quite low, ∼7–11 km s$^{-1}$, i.e. lower than the average

expansion velocity observed among AGB stars, which suggests that the high-velocity material found in the bipolar lobes should originate quite early on the AGB. This is consistent with the observation of a bipolar structure in the envelope of the AGB star Mira Ceti (Josselin et al. 2000b). KjPn 8 and M 1-16, the two youngest PNe according to their $M_{\rm m}/M_{\rm i}$ ratio, also display biconical extensions of the waist. Such structure does not appear in the older PN BV 5-1, probably because only the densest condensations of the molecular ring have survived to photodissociation by the stellar UV radiation.

While the PN shapes and structures have long been believed to result from the interaction of two rather spherical winds with enhancement of low density contrasts, it has been shown that the resulting bipolar structures are unstable (Livio & Pringle 1996). The observed geometries would rather result from the combined effects of binary interactions and a magnetohydrodynamical (MHD) collimation of the stellar winds (see García-Segura et al. 2001 and references therein). Indeed, according to these recent models three key-parameters have to be considered to examine the origin of the observed morphology: the rotation rate of the star during the AGB phase, the magnetic field and the ionizing flux of the post-AGB progenitor (García-Segura et al. 1999). The effects of stellar magnetic field seem not to be of prime importance. As stated by García-Segura et al. (1999), the degree of magnetic collimation decreases with increasing mass of the progenitor, and the progenitor of BV 5-1 should be massive ($\gtrsim$3–4 $M_{\odot}$), as it is a type I PN. Furthermore, the faint bipolar structure appears rather opened, but the collimation may have disappeared, as BV 5-1 is an evolved object. Then, rotation of the central star close to the disruption limit during the post-AGB phase may be the dominant process explaining the bipolarity. This high rotation could result from surface instabilities or merging of a binary system. Then the ionizing flux from the central star must play a key-role in the amplification of small-scale inhomogeneities in the AGB wind, especially as its expansion velocity is rather low, leading to the observed disrupted aspect. An additional phenomenon explaining these irregularities could be the disruption of the molecular envelope by jets, as observed in M 1-16 (Huggins et al. 2000).

Unfortunately, BV 5-1 is too far away to test such models with available observing facilities, as neither characteristic structures of MHD effects such as knots or filaments nor binarity of the central star are detectable. Further observations with infrared instrumentation on the Very Large Telescope (VLT), and much higher resolution CO mapping with the Atacama Large Millimeter Array (ALMA) should bring new constraints on the origins of these complex geometries.

*Acknowledgements.* We acknowledge the IRAM staff at Plateau de Bure and Grenoble for carrying out the observations, and for the competent help provided during the data reduction. We are also grateful to an anonymous referee for useful comments and suggestions which led to a significant improvement of the original manuscript. R. Bachiller acknowledges partial support from Spanish grant AYA 2000-927.

## References

Aaquist, O. B., & Kwok, S. 1990, A&AS, 84, 229
Bachiller, R., Huggins, P. J., Martin-Pintado, J., & Cox, P. 1992, A&A, 256, 231
Böhm-Vitense, E. 1956, PASP, 68, 430
Frank A. 2000, in Asymmetrical Planetary Nebulae II: From Origins to Microstructures, ed. J. H. Kastner, N. Soker, & S. Rappaport, ASP Conf. Ser., 199, 225
Forveille, T., Huggins, P. J., Bachiller, R., & Cox, P. 1998, ApJ, 495, L111
García-Segura, G., Franco, J. A., & López, J. A. 2001, RMxAA, in press
García-Segura, G., Langer, N., Różyczka, M., & Franco, J. A. 1999, ApJ, 517, 767
Gathier, R. 1987, A&AS, 71, 245
Guerrero, M. A., Villaver, E., Manchado, A., et al. 2000, ApJS, 127, 125
Guilloteau, S., Delannoy, J., Downes, D., et al. 1992, A&A, 262, 624
Huggins, P. J., Bachiller, R., Cox, P., & Forveille, T. 1996, A&A, 315, 284
Huggins, P. J., Forveille, T., Bachiller, R., & Cox, P. 2000, ApJ, 544, 889
Josselin, E., Bachiller, R., Manchado, A., & Guerrero, M. A. 2000a, A&A, 353, 363
Josselin, E., Mauron, N., Planesas, P., & Bachiller, R. 2000b, A&A, 362, 255
Kaler, J. B., Chu, Y.-H., & Jacoby, G. H. 1988, AJ, 96, 1407
Kastner, J. H., Weintraub, D. A., Gatley, I., et al. 1996, ApJ, 462, 777
Livio, M., & Pringle, J. E. 1996, ApJ, 465, L55
Manchado, A., Guerrero, M. A., Stanghellini, L., & Serra-Ricart, M. 1996, The IAC morphological catalog of northern galactic planetary nebulae
Mufson, S. L., Lyon, J., & Marionni, P. A. 1975, ApJ, 201, L85
Różyczka, M., & Franco, J. 1996, ApJ, 469, L127
Sahai, R., & Trauger, J. T. 1998, AJ, 116, 1357
Zweigle, J., Neri, R., Bachiller, R., et al. 1997, A&A, 324, 624